

Synthesis of Novel 1,4-dihydro-1,2,4,5-tetraarylpyrrolo[3,2-*b*]pyrroles Derivatives Catalyzed by NbCl₅ and Application in Dye Sensitized Solar Cells

Lucas Michelão Martins^{a*} , Bruna Andressa Bregadiolli^a, Laís Cristina Augusto^b,
José Henrique Lázaro de Carvalho^b, Maria Aparecida Zaghete^a, Luiz Carlos da Silva Filho^b

^aUniversidade Estadual Paulista (UNESP), Instituto de Química, 14800-060, Araraquara, SP, Brasil.

^bUniversidade Estadual Paulista (UNESP), Faculdade de Ciências, Departamento de Química, 17033-360, Bauru, SP, Brasil.

Received: January 06, 2021; Revised: May 11, 2021; Accepted: June 16, 2021

1,4-dihydro-1,2,4,5-tetraarylpyrrolo[3,2-*b*]pyrroles are a versatile class of materials with simple synthesis and promising application in organic electronic devices. In this work we present a method of synthesis of new 1,4-dihydro-1,2,4,5-tetraarylpyrrolo[3,2-*b*]pyrrole derivatives, with ester and carboxylic acid groups as anchoring groups, by multicomponent reactions using niobium pentachloride as catalyst. The new materials were structurally and optically characterized. Also, it was compared the bonding of different moieties to the titanium dioxide mesoporous film. The preliminary tests as dyes in standard configuration in dye-sensitized solar cells have shown a potential performance in the energy conversion.

Keywords: Lewis acid catalyst, Niobium, Heterocyclic dye, Dye-sensitized solar cells.

1. Introduction

1,4-dihydro-1,2,4,5-tetraarylpyrrolo[3,2-*b*]pyrroles represent a class of promising materials for application in organic electronics with interesting optoelectronic properties and great synthesis versatility, such as isolating them by a simple recrystallization¹⁻⁶. It is well known that the presence of a catalytic amount of a strong Lewis acid, such as *p*-toluenesulfonic acid or iron III salts (ferric chloride, ferric perchlorate and ferric triflate), improves the synthesis yield^{4,7}. NbCl₅, besides being highly electrophilic and acting as Lewis acid⁸, has low cost and has been used by our group and other researchers as an effective catalyst in synthetic methodologies in a variety of reactions including multicomponent reactions (MCR), with excellent results^{1,9,10}. As heteropentalenes, 1,4-dihydro-1,2,4,5-tetraarylpyrrolo[3,2-*b*]pyrroles belong to a class of heterocyclic compounds that have two fused pentagonal rings and the ones with 10 π electrons are aromatic². This structure has also been predicted as the most efficient electron donor among the 10 π electron systems¹¹. However, in the field of photoelectronics, the pyrrolo[3,2-*b*]pyrrole structure was very little explored, despite similar structures, mainly based on thiophenes, appearing in OLEDs¹² and in solar cells^{13,14} as hole transport in perovskites¹⁵ as well as dyes in dye sensitized solar cells (DSSCs)¹⁶. In recent years progress has been achieved through theoretical and experimental studies of photoelectronic properties and applications. The 1,4-dihydro-1,2,4,5-tetraarylpyrrolo[3,2-*b*]pyrroles usually have high absorption and emission in UV-vis region, and some investigations were made using various substituents on their aryl rings, showing good electronic

communication between the pyrrolo[3,2-*b*]pyrrole donor center and both the N-aryl and the C-aryl groups^{4,5,7}, with possibility of symmetry breaking of the excited state¹⁷⁻²¹, aggregation-induced and solid state emission²²⁻²⁶ and two-photon absorption²⁷⁻²⁹.

The 1,4-dihydro-1,2,4,5-tetraarylpyrrolo[3,2-*b*]pyrroles were also used to synthesize more complex structures with expanded π -systems, improving their photoelectronic properties^{4,6,7,24,27,29-37}. The formation of metal-organic frameworks between 1,4-dihydro-1,2,4,5-tetraarylpyrrolo[3,2-*b*]pyrroles and cadmium, gold, silver and zinc metals were published, with emission enhancement observed^{36,38,39}.

Dye-sensitized solar cells are photoelectrochemical devices that convert solar energy into electrical energy through redox reactions⁴⁰. DSSCs are constituted by a photoanode, a counter electrode and an electrolyte. In the photoanode, the dye is adsorbed in the titanium dioxide mesoporous film. The role of the dye is to absorb the photons from the sunlight and use their energy to excite electrons, injecting them into the TiO₂ conduction band, generating the charge transport in the device⁴¹. Consequently, a good dye would result in greater light energy conversion efficiency. For many years, the dyes based on ruthenium complexes (N719, N3) were the most common sensitizers with efficiency higher than 11% under AM 1.5 simulated sunlight⁴². However, the efficiency of devices with these sensitizers has remained stagnant in recent years. The advance of metal-free dyes, with porphyrins for instance, have overcome the efficiency of the metal-based dyes in DSSC achieving 10% efficiency in the same insulation conditions^{43,44}. Dominguez *et al.*⁴⁵ have applied pyrrolo[3,2-*b*]pyrrole central core molecules with configuration acceptor-

*e-mail: lm.martins@unesp.br

donor-acceptor as electron donor in organic solar cells. In his work he achieved the open-circuit voltage of 0.99 V. Also, Wang and co-workers³⁵ have synthesized organic dyes based on 1,4-dihydro-1,2,4,5-tetraarylpyrrolo[3,2-*b*]pyrroles with incorporation of different conjugated bridges and conjugated groups, such as thiophenes, achieving conversion efficiencies as high as 6.56% in DSSCs.

Herein, we present a method for the synthesis of new 1,4-dihydro-1,2,4,5-tetraarylpyrrolo[3,2-*b*]pyrrole derivatives by multicomponent reactions employing niobium pentachloride as catalyst as well as its structural and optical characterization and tested in standard configuration in DSSCs.

2. Experimental

All the reactions were performed using anhydrous acetonitrile. The chemicals were purchased from Sigma-Aldrich Chemical Co. (St. Louis, MO, USA) and used without further purification.

Thin-layer chromatography was performed on 0.2 mm Merck 60 F254 silica gel aluminum sheets, which were visualized with a phosphomolybdic acid/ammonium cerium (IV) sulfate/water/sulfuric acid mixture. Bruker DRX 400 spectrometer was used for the NMR spectra (CDCl₃ solutions) using TMS as internal reference for ¹H and CDCl₃ as an internal reference for ¹³C. A Jasco FTIR model 4600 was used to record IR spectra (KBr pellets). UV-vis spectra were recorded in an Agilent Technologies Cary 8454 and fluorescence spectra in a SpectraMax M2, from Molecular Devices, both in room temperature with a 10 mm quartz cuvette and dichloromethane as solvent. Fluorescence emission spectra were obtained using a Synergy2 Multi-Mode reader (BioTek, USA).

Quantum yields were analyzed by adjusting the solution absorption using the UV-vis to ca. 0.05 at 320-410 nm wavelength, the output was measured using the luminescence spectrophotometer at the same wavelength and comparing it to the known 9,10-diphenylanthracene standard using Equation 1:

$$\Phi_f = \Phi_{std} \times \frac{A_{std}F}{AF_{std}} \times \frac{n^2}{n_{std}^2} \quad (1)$$

Φ is the fluorescence quantum yield, A is the absorption of the excitation wavelength, F is the area under the emission curve, and n is the refractive index of the solvents used. Subscript std denotes the standard. The compounds were solubilized in ethanol and the concentration maintained at about 1.0×10^{-6} M to follow the protocol for analysis.

DSSCs were made by using glass coated with fluorine-doped tin oxide (FTO Sigma-Aldrich $7\Omega/\square$) as transparent conducting electrode (TCO). The substrates were cleaned by consecutive sonication in Extran (Merck), water, acetone and isopropanol in an ultrasonic bath (Unique) and dried in nitrogen flux. The photoanode films were prepared with TiO₂ commercial transparent paste (DYERS) deposited by screen-printing method using a mold with 0.5×0.5 cm² and 10 μ m thickness. The films were sintered at 450 °C for 30 min to eliminate organic compounds from the paste and followed by immersion at 80 °C in the solution of dye. To determine

the dye loading time, UV-vis absorption technique was used. The concentration of the absorbed dye as function of immersion time, after the desorption with NaOH alcoholic solution, is presented in the Supporting Information (Table S1). Hence, 2 h immersion was used in dichloromethane solution. The counter electrode used was made depositing a solution of H₂PtCl₆ in ethanol in FTO and sintered at 200 °C for 30 min. The two electrodes were sandwiched with the electrolyte (DYERSBV12), using parafilm M as a spacer, with a separation distance of approximately 0.13 mm. The characterization of the devices was performed in ambient atmosphere using a Keithley 2400 source meter unit and an Oriol xenon lamp (450W) coupled with an AM 1.5 filter as light source. The light intensity of 100 mWcm⁻² was used in all measurements. Devices parameters were tested for at least three devices for each sample. V_{max} and J_{max} are, respectively, the potential and the current density at which electric power generated by the cell is maximum (P_{max}).

The fill factor given by Equation 2:

$$FF = \frac{V_{max}J_{max}}{V_{oc}J_{sc}} \quad (2)$$

J_{sc} (A/cm²) is the short circuit photo-current ($V = 0$) and V_{oc} (V) is the open circuit voltage ($J = 0$).

2.1. General procedure for the synthesis of 1,4-dihydro-1,2,4,5-tetraarylpyrrolo[3,2-*b*]pyrrole derivatives

For a solution of niobium pentachloride (0.250 mmol) in 1.0 mL of anhydrous acetonitrile, maintained at room temperature in a capped flask, it was added a solution of benzaldehyde derivative (**1a-b**) (2.0 mmol), aniline derivative (**2a-b**) (2.0 mmol) and butane-2,3-dione (**3**) (1.0 mmol) in 5 mL in anhydrous acetonitrile. After the addition was completed, stirring was continued at room temperature until the end of the reaction (20 to 40 min followed by TLC – 1:1 hexane:dichloromethane). The reaction mixture was quenched with water (3.0 mL). The mixture was extracted with dichloromethane (10.0 mL). The organic layer was separated and washed with saturated sodium bicarbonate solution (3 \times 10.0 mL), saturated brine (2 \times 10.0 mL), and then dried over anhydrous MgSO₄. The solvent was removed under vacuum and the resulting mixture was dissolved in boiling ethyl acetate (1.0 mL) that, upon cooling, resulted in a yellow solid. This solid was recrystallized in ethyl acetate to obtain a yellowish solid.

2.1.1. Dimethyl 4,4'-(1,4-di-*p*-tolyl-1,4-dihydropyrrolo[3,2-*b*]pyrrole-2,5-diyl)dibenzoate (**4a**)

NMR-¹H (600 MHz, (CD₃)₂SO): δ (ppm) 7.81 (AA'XX', 4H), 7.33 (AA'XX', 4H), 7.27 (AA'XX', 4H), 7.18 (AA'XX', 4H), 6.60 (s, 2H), 3.82 (s, 6H), 2.35 (s, 6H). NMR-¹³C (150 MHz, (CD₃)₂SO): δ (ppm) 166.4 (C=O), 137.2 (C), 136.9 (C), 136.1 (C), 135.4 (C), 133.0 (C), 130.5 (CH), 130.1 (C), 129.8 (CH), 127.7 (CH), 125.4 (CH), 96.3 (CH), 49.06 (CH₃), 21.2 (CH₃). IR (ν_{max} /cm⁻¹): 1711, 1605, 1513, 1273, 1190. MP 305-307 °C.

2.1.2. Dimethyl 4,4'-(2,5-di([1,1'-biphenyl]-4-yl)pyrrolo[3,2-*b*]pyrrole-1,4-diyl)dibenzoate (**4b**)

NMR-¹H (600 MHz, (CD₃)₂SO): δ(ppm) 7.96 (AA'XX', 4H), 7.77 (AA'XX', 4H), 7.38-7.34 (m, 10H), 7.29 (AA'XX', 4H), 7.22-7.19 (m, 4H), 3.84 (s, 6H). NMR-¹³C (150 MHz, (CD₃)₂SO): δ(ppm) 167.9 (C=O), 139.8 (C), 138.8 (C), 135.2 (C), 132.6 (C), 132.2 (C), 130.1 (CH), 129.4 (CH), 128.4 (CH), 127.9 (CH), 127.1 (CH), 126.9 (CH), 126.0 (CH), 97.3 (CH), 52.8 (CH₃). IR (ν_{max}/cm⁻¹): 1712, 1603, 1510, 1413, 1275, 1110, 765. MP 320-322 °C.

2.2. General procedure for the hydrolysis reaction of the ester groups of 1,4-dihydro-1,2,4,5-tetraarylpyrrolo[3,2-*b*]pyrrole derivatives

The 1,4-dihydro-1,2,4,5-tetraarylpyrrolo[3,2-*b*]pyrrole derivative (**4a-4b**) (0.50 mmol) was solubilized in ethanol (2.0 mL) followed by the addition of sodium hydroxide 5M (0.2 mL). The reaction was stirred at reflux for 12 h. The reaction was quenched with water (2.0 mL) and after cooling to the room temperature, the pH was adjusted to 5 using a HCl solution 2M, where the product precipitation occurred. The product was recovered by filtration as a yellow solid. It was recrystallized in ethyl acetate and a pale yellow solid was obtained.

2.2.1. 4,4'-(1,4-di-*p*-tolyl-1,4-dihydropyrrolo[3,2-*b*]pyrrole-2,5-diyl)dibenzoic acid (**5a**)

NMR-¹H (600 MHz, (CD₃)₂SO): δ(ppm) 7.79 (AA'XX', 4H), 7.3 (AA'XX', 4H), 7.27 (AA'XX', 4H), 7.18 (AA'XX', 4H), 6.58 (s, 2H), 2.36 (s, 6H). NMR-¹³C (150 MHz, (CD₃)₂SO): δ(ppm) 166.4 (C=O), 137.2 (C), 136.9 (C), 136.1 (C), 135.4 (C), 133.0 (C), 130.5 (CH), 130.1 (C), 129.8 (CH), 127.7 (CH), 125.4 (CH), 96.3 (CH), 21.2 (CH₃). IR (ν_{max}/cm⁻¹): 1686, 1603, 1513, 1379, 1274. MP 328-330 °C.

2.2.2. 4,4'-(2,5-di([1,1'-biphenyl]-4-yl)pyrrolo[3,2-*b*]pyrrole-1,4-diyl)dibenzoic acid (**5b**)

NMR-¹H (600 MHz, (CD₃)₂SO): δ(ppm) 8.01 (AA'XX', 4H), 7.69 (AA'XX', 4H), 7.64 (AA'XX', 4H), 7.46-7.43 (m, 10H), 7.32 (AA'XX', 4H), 6.71 (s, 2H), 4.11 (sl, 2H). NMR-¹³C (150 MHz, (CD₃)₂SO): δ(ppm) 167.3 (C=O), 139.8 (C), 138.4 (C), 135.6 (C), 132.3 (C), 132.0 (C), 131.2 (CH), 129.4 (CH), 128.6 (CH), 127.9 (CH), 127.1 (CH), 126.9 (CH), 125.0 (CH), 97.3 (CH). IR (ν_{max}/cm⁻¹): 1685, 1603, 1511, 1413, 1275, 1111, 762. MP 330-331 °C.

3. Results and Discussion

To achieve an enhanced performance of organic electronic devices it is well known that a good contact in the interface between inorganic semiconductors and organic compounds is essential. Accordingly, there are many strategies to obtain better charge transfer process, such as a covalent bond between the organic and inorganic materials. Hence, the original goal was the synthesis of the 1,4-dihydro-1,2,4,5-tetraarylpyrrolo[3,2-*b*]pyrrole derivatives with the presence of -COOH groups as anchoring groups for TiO₂ in DSSCs⁴⁶. The dyes synthesized have the donor-π-acceptor configuration,

with the pyrrolo[3,2-*b*]pyrrole as donor centrum, and the carboxylic acid as both the acceptor and anchoring group.

The synthetic route used was an optimized synthetic procedure using NbCl₅ as catalyst that we have previously developed¹. This synthetic procedure is based on the multicomponent reaction between an aniline derivative, a benzaldehyde derivative and the 2,3-butanedione, catalysed by niobium pentachloride in mild conditions, using ambient temperature and air atmosphere. This procedure has some interesting characteristics. For instance, reactions with niobium pentachloride usually are done under nitrogen atmosphere, as the NbCl₅ reacts easily with the water present in the air, but in this procedure, due to the small reaction time and the oxidation step, the reaction occurs well in ambient atmosphere. Another advantage of this method using NbCl₅ catalyst over other methods for the synthesis of 1,4-dihydro-1,2,4,5-tetraarylpyrrolo[3,2-*b*]pyrrole derivatives is the absence of heating. In addition, the reaction product is not soluble in the reaction solvent, acetonitrile, thus it precipitates in the reaction flask, which permit the product formation by shifting the chemical equilibrium and allowing easy recovery and purification of the product, by recrystallization. The recrystallization process is easy, solubilizing the organic phase in hot ethyl acetate and allowing it to cool gives the product with few impurities, that are washed with cold ethyl acetate to afford the pure product in good yield.

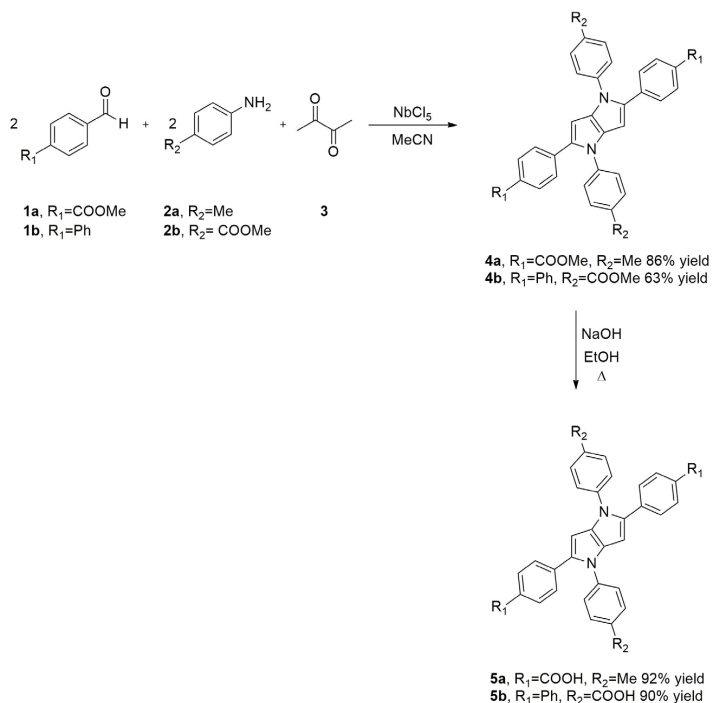
In order to obtain carboxylic acid anchoring groups in the 1,4-dihydro-1,2,4,5-tetraarylpyrrolo[3,2-*b*]pyrrole derivatives, firstly it was obtained 1,4-dihydro-1,2,4,5-tetraarylpyrrolo[3,2-*b*]pyrrole derivatives with ester groups, followed by the ester hydrolysis, obtaining the desired carboxylic acid derivatives.

The results of the synthesis are summarized in Scheme 1.

As can be seen in Scheme 1, the procedure is very efficient, with high yields in low reaction times. The groups in the *para* position of aniline and benzaldehyde derivatives have a significant effect in the product yield. The difference in yield can be attributed to the competition between the desired reaction and a side-reaction that form imidazole derivatives². Our previous work has shown a correlation of the difference between the local softness of the carbonyl in the aldehyde and the diketone oxygens with the experimental yields, indicating that reactions where there is lower probability of interaction between compounds **1** and **3** have higher yields¹.

To hydrolyze the ester group to a carboxylic acid, an easy process developed by Kikuchi was successfully used (Scheme 1). This process uses ethanol as solvent, and a sodium hydroxide solution (5,0 M) to cleave the ester group, under heating for 12 h. The hydrolysis reaction had great yields (Scheme 1), and the purification was easy and fast by a simple filtration followed by recrystallization in ethyl acetate.

After the synthesis, the optical characterization of the compounds was performed. Dichloromethane was chosen as solvent due to the better solubility. The results of the carboxylic acids derivatives were compared with the esters derivatives, to evaluate their behavior and changes (Figure 1a, 1b and Table 1).



Scheme 1. Synthesis of 1,4-dihydro-1,2,4,5-tetraarylpyrrolo[3,2-*b*]pyrrole derivatives.

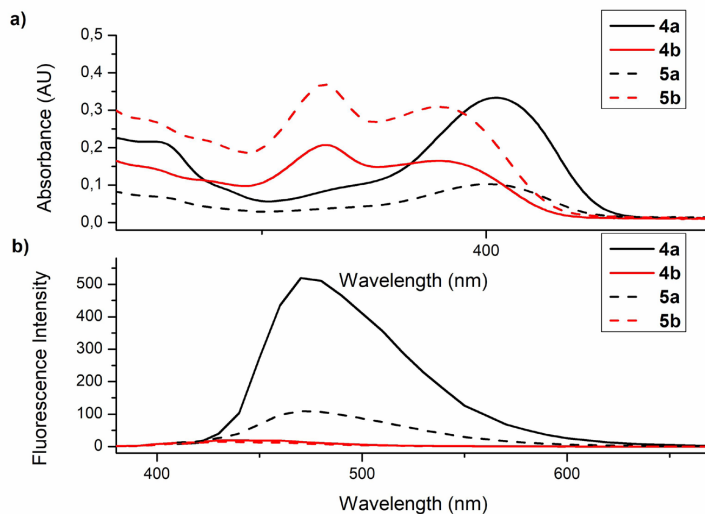


Figure 1. a) UV-vis absorption spectra and b) fluorescence spectra of the compounds **4a**, **4b**, **5a** and **5b** ($1,0 \times 10^{-5}$ M, CH_2Cl_2).

Table 1. Spectroscopic data for the compounds **4a**, **4b**, **5a**, and **5b**.

| Compound | λ_{abs} (nm) | λ_{em} (nm) | Stokes shift (nm) | ϵ ($\text{M}^{-1} \text{cm}^{-1}$) | Φ^1 |
|-----------|-----------------------------|----------------------------|-------------------|---|----------|
| 4a | 405 | 470 | 65 | $3,3 \times 10^5$ | 0,59 |
| 4b | 328 | 440 | 112 | $2,1 \times 10^5$ | 0,10 |
| 5a | 402 | 470 | 68 | $1,0 \times 10^5$ | 0,34 |
| 5b | 328 | 430 | 102 | $3,7 \times 10^5$ | 0,12 |

¹ Determined using 9,10-diphenylanthracene in ethanol ($1,0 \times 10^{-5}$ M) as standard

Analyzing the optical results for the 1,4-dihydro-1,2,4,5-tetraarylpyrrolo[3,2-*b*]pyrrole acid derivatives, one can observe that there was no significant change in the absorption wavelengths of the compounds. Considering that the structural

change is the removal of a methyl group, no noticeable change was expected. The coefficients of molar absorptivity remained high. A drop in the quantum yield was observed for compound **5a** as compared to **4a**, possibly due to methyl

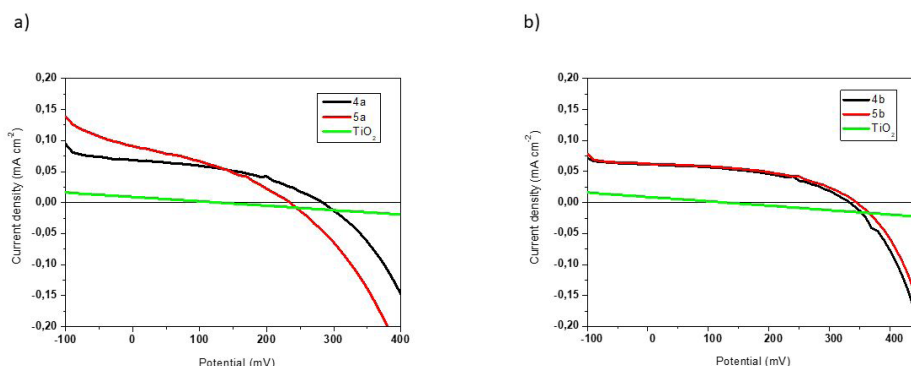


Figure 2. JxV curves for the DSSCs made with the 1,4-dihydro-1,2,4,5-tetraarylpyrrolo[3,2-*b*]pyrrole derivatives **4a**, **4b**, **5a**, **5b**.

Table 2. Photovoltaic performance data for the compounds **4a**, **4b**, **5a**, and **5b**.

| Compound | V_{oc} (V) | J_{sc} (mA/cm ²) | FF |
|---------------|--------------|--------------------------------|----|
| 4a | 0.327 | 0.064 | 51 |
| 5a | 0.284 | 0.088 | 41 |
| 4b | 0.334 | 0.061 | 49 |
| 5b | 0.344 | 0.067 | 49 |
| No dye | 0.107 | 0.008 | 20 |

groups that stabilize the excited state of molecule **4a**, whereas hydrogen does not stabilize the excited state of compound **4a**. In the case of compounds **4b** and **5b** there was no significant difference, probably due to the increase in conjugation of the phenyl group, which is greater than with the methyl group.

After performing the synthesis and characterization, the tests for the use of **4a**, **4b**, **5a** and **5b** compounds in dye-sensitized solar cells were performed. To test the best dye loading condition, the TiO₂ anode was immersed in the dye solution (3,0 x 10⁻³ M) and the adsorption was measured each hour until 3 hours and then after 24h. In all cases the adsorption had its maximum in 2 h of immersion, and in 24 h the adsorption was equal or slightly lower, indicating the possibility of an aggregation and/or desorption of the dye over time as seen in Supplementary Material Table S1. We have used a platinum counter electrode deposited in FTO and an electrolyte with the I⁻/I₃⁻ redox pair. The device was assembled as photoanode: electrolyte: counter electrode.

In the DSSC system, the photoelectron is generated in the core of the pyrrolo[3,2-*b*]pyrrole and injected from the singlet excited state of the dye to the TiO₂ conduction band thru the anchoring group. The resulting cation produced in this photo-induced injection is reduced by the electrolyte and at the counter electrode, the Pt reduces the oxidized electrolyte, leading to the photocurrent generation in the device. Herein, the performance of the device under influence of two different radicals (phenyl and methyl), the position and the anchoring group will be analyzed. The JxV curves are presented in Figure 2 in comparison with TiO₂ with no dye adsorbed. The photovoltaic performance and data are presented in Table 2.

The photovoltaic performance was similar for both ester and carboxylic acid structures. Analyzing the dye loading

values (Table S1) is possible to observe that the carboxylic groups did not improve the anchoring of the molecules in the oxide as was expected, with the adsorption values very similar to the ester compounds. As can be seen in the literature, there are reports about the anchoring in the metal from other oxygen containing groups, such as phosphonic acid and catechol⁴⁷. It is possible to assume that the ester groups are acting as strong ester linkage with the TiO₂ surface (Figure S1). Both carboxyl and ester groups, in this case, enables good electronic communication and electron acceptance.

The V_{oc} is a property dependent on the energy of the band gap of each material. It was observed better V_{oc} in the compounds **4b** and **5b**. The higher J_{sc} is obtained for the compound **5a**, probably due to the probability of charge generation processes, but it is necessary more studies to confirm this hypothesis, such as investigation of passivation of the surface of the absorber and the lifetime of the minority carriers. The FF is a property dependent on the V_{oc} and I_{sc} values.

Despite the low efficiencies, calculated as 0.01% for all the dyes, these results showed their potential as sensitizer dyes for solar cells. Wang and coworkers showed good results (4.16-6.56% efficiency) with similar, but more complex dyes, in different standard conditions, using 0.6 M dimethylpropyl imidazolium iodide, 0.1 M lithium iodide, 0.05 M iodine and 0.5 M tert-butylpyridine in acetonitrile/3-methoxypropionitrile (85:15, v/v), as electrolyte. They also used the co-adsorbent chenodeoxycholic acid to improve the cell performance³⁵. Li and coworkers also used similar dyes, with a thienothiophene core, with 3.87% efficiency in different standard conditions, using 0.05 M I₂, 0.1 M LiI, 0.6 M 1-propyl-3-methylimidazolium iodide and 0.5 M 4-tert-butylpyridine in a mixed solvent of acetonitrile and valeronitrile (1:1, v/v) as electrolyte and also using co-adsorbent chenodeoxycholic acid to prevent dye aggregation on TiO₂ surface⁴⁸. (Another work using thienothiophene core was described by Ho and coworkers, achieving 5.25% efficiency using a 0.6 M 1,2-dimethyl-3-propylimidazolium iodide, 0.1 M LiI, 0.05 M I₂ acetonitrile and 4-tert-butylpyridine (volume ratio, 1:1) electrolyte⁴⁹.)

It is important to note that the device results are preliminary, and the performance could be improved accordingly with changes in the oxide thickness and/or electrolyte used, for example. The intention of this work is to show the potential of the material for organic electronic applications.

4. Conclusion

In conclusion, it was possible to synthesize new 1,4-dihydro-1,2,4,5-tetraarylpyrrolo[3,2-*b*]pyrrole derivatives with ester and carboxylic acid groups with high yield and low reaction times. These compounds were characterized and, due to its presented potential, tested as sensitizer dyes in solar cells. It was observed a good electronic communication between the ester group and the titanium oxide, similar to the carboxylic acid group interaction. The preliminary devices showed that these compounds have potential for organic electronic applications, with some adjustments in conditions and structure, depending on the desired application.

5. Acknowledgments

This study was financed in part by the Coordenação de Aperfeiçoamento de Pessoal de Nível Superior - Brasil (CAPES) - Finance Code 001. The authors would like to thank Fundação de Amparo à Pesquisa do Estado de São Paulo (FAPESP 2016/01599-1, 2017/07627-0, 2018/09235-4 and 2018/14506-7), Conselho Nacional de Desenvolvimento Científico e Tecnológico (CNPq) (Proc. 302769/2018-8) and Pró-Reitoria de Pesquisa da UNESP (PROPe-UNESP) for their financial support. The authors would also like to thank CBMM – Companhia Brasileira de Metalurgia e Mineração for the NbCl₅ samples.

6. References

- Martins LM, de Faria Vieira S, Baldacim GB, Bregadiolli BA, Caraschi JC, Batagin-Neto A, et al. Improved synthesis of tetraaryl-1,4-dihydropyrrolo[3,2-*b*]pyrroles a promising dye for organic electronic devices: An experimental and theoretical approach. *Dye Pigment*. 2018 Jan;148:81-90. <http://dx.doi.org/10.1016/j.dyepig.2017.08.056>.
- Janiga A, Glodkowska-Mrowka E, Stoklosa T, Gryko DT. Synthesis and optical properties of tetraaryl-1,4-dihydropyrrolo[3,2-*b*]pyrroles. *Asian J Org Chem*. 2013;2(5):411-5. <http://doi.wiley.com/10.1002/ajoc.201200201>.
- Krzyszewski M, Gryko D, Gryko DT. The tetraarylpyrrolo[3,2-*b*]pyrroles: from serendipitous discovery to promising heterocyclic optoelectronic materials. *Acc Chem Res*. 2017;50(9):2334-45. <http://dx.doi.org/10.1021/acs.accounts.7b00275>.
- Tasior M, Koszarna B, Young DC, Bernard B, Jacquemin D, Gryko D, et al. Fe(iii)-Catalyzed synthesis of pyrrolo[3,2-*b*]pyrroles: formation of new dyes and photophysical studies. *Org Chem Front*. 2019;6(16):2939-48.
- Banasiewicz M, Stężycki R, Kumar GD, Krzyszewski M, Tasior M, Koszarna B, et al. Electronic communication in pyrrolo[3,2-*b*]pyrroles possessing sterically hindered aromatic substituents. *Eur J Org Chem*. 2019;2019(31-32):5247-53.
- Stężycki R, Reger D, Hoelzel H, Jux N, Gryko DT. Synthesis and photophysical properties of hexaphenylbenzene-Pyrrolo[3,2-*b*]pyrroles. *Synlett*. 2018;29(19):2529-34.
- Krzyszewski M, Gryko D, Gryko DT. The tetraarylpyrrolo[3,2-*b*]pyrroles: from serendipitous discovery to promising heterocyclic optoelectronic materials. *Acc Chem Res*. 2017;50(9):2334-45.
- Lacerda V Jr, Santos DA, da Silva-Filho LC, Greco SJ, Santos RB. The growing impact of niobium in organic synthesis and catalysis. *Aldrichimica Acta*. [serial on the Internet]. 2012;45(1):19-27. [cited 2018 Mar 1]. Available from: <https://www.sigmaaldrich.com/deepweb/assets/sigmaaldrich/marketing/global/documents/694/791/acta-45-1.pdf>
- Arpini B, Andrade Bartolomeu A, Andrade C, da Silva-Filho L, Lacerda V. Recent advances in using niobium compounds as catalysts in organic chemistry. *Curr Org Synth*. 2015;12(5):570-83. <http://dx.doi.org/10.2174/157017941205150821125817>.
- da Silva BHST, Bregadiolli BA, Graeff CF O, da Silva-Filho LC. NbCl₅-promoted synthesis of fluorescein dye derivatives: spectroscopic and spectrometric characterization and their application in dye-sensitized solar cells. *Chempluschem*. 2017;82(2):261-9. <http://doi.wiley.com/10.1002/cplu.201600530>.
- Tanaka S, Kumagai T, Mukai T, Kobayashi T. 1,4-Dihydropyrrolo[3,2-*b*]pyrrole: the electronic structure elucidated by photoelectron spectroscopy. *Bull Chem Soc Jpn*. 1987;60(6):1981-3.
- Evensohn SJ, Mumm MJ, Pokhodnya KI, Rasmussen SC. Highly fluorescent Dithieno[3,2-*b*:2',3'-*d*]pyrrole-based materials: synthesis, characterization, and OLED device applications. *Macromolecules*. 2011;44(4):835-41. <http://dx.doi.org/10.1021/ma102633d>.
- Kast H, Mishra A, Schulz GL, Urdanpilleta M, Mena-Osteritz E, Bäuerle P, et al. N-Heteropentacenes of Different Conjugation Length: Structure–Property Relationships and Solar Cell Performance. *Adv Funct Mater*. 2015;25(22):3414-24. <http://dx.doi.org/10.1002/adfm.201500565>.
- Mishra A, Popovic D, Vogt A, Kast H, Leitner T, Walzer K, et al. A–D–A-type S_N-heteropentacenes: next-generation molecular donor materials for efficient vacuum-processed organic solar cells. *Adv Mater*. 2014;26(42):7217-23. <http://dx.doi.org/10.1002/adma.201402448>.
- Qin P, Kast H, Nazeeruddin MK, Zakeeruddin SM, Mishra A, Bäuerle P, et al. Low band gap S_N-heteroacene-based oligothiophenes as hole-transporting and light absorbing materials for efficient perovskite-based solar cells. *Energy Environ Sci*. 2014;7(9):2981-5. <https://doi.org/10.1039/C4EE01220H>.
- Jung JW, Jo JW, Jung EH, Jo WH. Recent progress in high efficiency polymer solar cells by rational design and energy level tuning of low bandgap copolymers with various electron-withdrawing units. *Org Electron*. 2016;31:149-70. <https://doi.org/10.1016/j.orgel.2016.01.034>.
- Dereka B, Vauthey E. Direct local solvent probing by transient infrared spectroscopy reveals the mechanism of hydrogen-bond induced nonradiative deactivation. *Chem Sci (Camb)*. 2017;8(7):5057-66.
- Dereka B, Vauthey E. Solute-solvent interactions and excited-state symmetry breaking: beyond the dipole-dipole and the hydrogen-bond interactions. *J Phys Chem Lett*. 2017;8(16):3927-32.
- Dereka B, Rosspeintner A, Stężycki R, Ruckebusch C, Gryko DT, Vauthey E. Excited-state symmetry breaking in a quadrupolar molecule visualized in time and space. *J Phys Chem Lett*. 2017;8(24):6029-34.
- Dereka B, Helbing J, Vauthey E. Transient glass formation around a quadrupolar photoexcited dye in a strongly H-bonding liquid observed by transient 2D-IR spectroscopy. *Angew Chem Int Ed*. 2018;57(52):17014-8.
- Dereka B, Furera J, Rosspeintner A, Vauthey E. Halogen-bond assisted photo induced electron transfer. *Molecules*. 2019;24(23):4361.
- Sadowski B, Hassanein K, Ventura B, Gryko DT. Tetraphenylethylenepyrrolo[3,2-*b*]pyrrole Hybrids as solid-state emitters: the role of substitution pattern. *Org Lett*. 2018;20(11):3183-6.
- Peng Z, Ji Y, Huang Z, Tong B, Shi J, Dong Y. A strategy for the molecular design of aggregation-induced emission units further modified by substituents. *Mater Chem Front*. 2018;2(6):1175-83.
- Ma Y, Zhang Y, Kong L, Yang J. Mechanoresponsive material of AIE-active 1,4-dihydropyrrolo[3,2-*b*]pyrrole luminophores bearing tetraphenylethylene group with rewritable data storage. *Molecules*. 2018;23(12):1-10.

25. Li K, Liu Y, Li Y, Feng Q, Hou H, Tang BZ. 2,5-bis(4-alkoxycarbonylphenyl)-1,4-diaryl-1,4-dihydropyrrolo[3,2-*b*]pyrrole (AAPP) AIEgens: tunable RIR and TICT characteristics and their multifunctional applications. *Chem Sci (Camb)*. 2017;8(10):7258-67.
26. Dai S, Cai Z, Peng Z, Wang Z, Tong B, Shi J, et al. A stabilized lamellar liquid crystalline phase with aggregation-induced emission features based on pyrrolopyrrole derivatives. *Mater Chem Front*. 2019;3(6):1105-12.
27. Liu H, Ye J, Zhou Y, Fu L, Lu Q, Zhang C. New pyrrolo[3,2-*b*]pyrrole derivatives with multiple-acceptor substitution: efficient fluorescent emission and near-infrared two-photon absorption. *Tetrahedron Lett*. 2017;58(52):4841-4.
28. Łukasiewicz ŁG, Ryu HG, Mikhaylov A, Azarias C, Banasiewicz M, Kozankiewicz B, et al. Symmetry Breaking in Pyrrolo[3,2-*b*]pyrroles: Synthesis, Solvatofluorochromism and Two-photon Absorption. *Chem Asian J*. 2017;12(14):1736-48.
29. Tasior M, Hassanein K, Mazur LM, Sakellari I, Gray D, Farsari M, et al. The role of intramolecular charge transfer and symmetry breaking in the photophysics of pyrrolo[3,2-*b*]pyrrole-dione. *Phys Chem Chem Phys*. 2018;20(34):22260-71.
30. Bardi B, Krzeszewski M, Gryko DT, Painelli A, Terenziani F. Excited-state symmetry breaking in an aza-nanographene dye. *Chemistry*. 2019;25(61):13930-8.
31. Benkyi I, Staszewska-Krajewska O, Gryko DT, Jaszunski M, Stanger A, Sundholm D. Interplay of aromaticity and antiaromaticity in N-Doped nanographenes. *J Phys Chem A*. 2020;124(4):695-703.
32. Krzeszewski M, Sahara K, Poronik YM, Kubo T, Gryko DT. Unforeseen 1,2-aryl shift in Tetraarylpyrrolo[3,2-*b*]pyrroles triggered by oxidative aromatic coupling. *Org Lett*. 2018;20(6):1517-20.
33. Ryu HG, Mayther MF, Tamayo J, Azarias C, Espinoza EM, Banasiewicz M, et al. Bidirectional solvatofluorochromism of a pyrrolo[3,2-*b*]pyrrole-Diketopyrrolopyrrole Hybrid. *J Phys Chem C*. 2018;122(25):13424-34.
34. Tasior M, Czichy M, Łapkowski M, Gryko DT. Dibenzothienopyrrolo[3,2-*b*]pyrrole: the missing member of the thienoacene family. *Chem Asian J*. 2018;13(4):449-56.
35. Wang J, Chai Z, Liu S, Fang M, Chang K, Han M, et al. Organic dyes based on tetraaryl-1,4-dihydropyrrolo-[3,2-*b*]pyrroles for photovoltaic and photocatalysis applications with the suppressed electron recombination. *Chemistry*. 2018;24(68):18032-42.
36. Wei Z, Wu XH, Luo P, Wang JY, Li K, Zang SQ. Matrix coordination induced emission in a three-dimensional silver cluster-assembled. *Mater Chem*. 2019;25(11):2750-6.
37. Wu D, Zheng J, Xu C, Kang D, Hong W, Duan Z, et al. Phosphindole fused pyrrolo[3,2-*b*]pyrroles: A new single-molecule junction for charge transport. *Dalton Trans*. 2019;48(19):6347-52.
38. Hawes CS, Mille GMO, Byrne K, Schmitt W, Gunnlaugsson T. Tetraarylpyrrolo[3,2-*b*]pyrroles as versatile and responsive fluorescent linkers in metal-organic frameworks. *Dalton Trans*. 2018;47(30):10080-92.
39. Purba PC, Bhattacharyya S, Maity M, Mukhopadhyay S, Howlader P, Mukherjee PS. Linkage induced enhancement of fluorescence in metal-carbene bond directed metallacycles and metallacages. *Chem Commun (Camb)*. 2019;55(57):8309-12.
40. Gratzel M. Photoelectrochemical cells. *Nature*. 2001;414(6861):338-44. <https://doi.org/10.1038/35104607>.
41. Ye M, Wen X, Wang M, Iocozzia J, Zhang N, Lin C, et al. Recent advances in dye-sensitized solar cells: from photoanodes, sensitizers and electrolytes to counter electrodes. *Mater Today*. 2015;18(3):155-62. <https://doi.org/10.1016/j.mattod.2014.09.001>.
42. Selopal GS, Wu H-P, Lu J, Chang Y-C, Wang M, Vomiero A, et al. Metal-free organic dyes for TiO₂ and ZnO dye-sensitized solar cells. *Sci Rep*. 2016;6:18756. <https://doi.org/10.1038/srep18756>.
43. Joly D, Pellejà L, Narbey S, Oswald F, Chiron J, Clifford JN, et al. A robust organic dye for dye sensitized solar cells based on iodine/iodide electrolytes combining high efficiency and outstanding stability. *Sci Rep*. 2014;4:4033. <https://doi.org/10.1038/srep04033>.
44. Higashino T, Imahori H. Porphyrins as excellent dyes for dye-sensitized solar cells: recent developments and insights. *Dalton Trans*. 2015;44(2):448-63. <https://doi.org/10.1039/C4DT02756F>.
45. Domínguez R, Montcada NF, de la Cruz P, Palomares E, Langa F. Pyrrolo[3,2-*b*]pyrrole as the central core of the electron donor for solution-processed organic solar cells. *ChemPlusChem*. 2017;82(7):1096-104. <https://doi.org/10.1002/cplu.201700158>.
46. Kim B-G, Chung K, Kim J. Molecular design principle of all-organic dyes for dye-sensitized solar cells. *Chemistry*. 2013;19(17):5220-30. <https://doi.org/10.1002/chem.201204343>.
47. Zhang L, Cole JM. Anchoring groups for dye-sensitized solar cells. *ACS Appl Mater Interfaces*. 2015;7(6):3427-55. <https://doi.org/10.1021/am507334m>.
48. Li S-L, Jiang K-J, Shao K-F, Yang L-M. Novel organic dyes for efficient dye-sensitized solar cells. *Chem Commun (Camb)*. 2006;(26):2792-4. <https://doi.org/10.1039/B603706B>.
49. Ho P-Y, Wang Y, Yiu S-C, Kwok Y-Y, Siu C-H, Ho C-L, et al. Photophysical characteristics and photosensitizing abilities of thieno[3,2-*b*]thiophene-Based photosensitizers for photovoltaic and photocatalytic applications. *J Photochem Photobiol Chem*. 2021;406:112979. <https://doi.org/10.1016/j.jphotochem.2020.112979>.

Supplementary Material

The following online material is available for this article:

Table S1 - Dye adsorption concentration in TiO₂ over time.

Figure S1 - FTIR comparison between free and TiO₂-adsorbed dyes.